Chemical etching of boron-rich layer and its impact on high efficiency n-type silicon solar cells

Kyungsun Ryu,[1] Ajay Upadhyaya,[1] Hyun-Jin Song,[2] Chel-Jong Choi,[2,3] Ajeet Rohatgi,[1] and Young-Woo Ok[1,a)]
[1]*School of Electrical and Computer Engineering, Georgia Institute of Technology, 777 Atlantic Drive, Atlanta, Georgia 30332-0250, USA*
[2]*School of Semiconductor and Chemical Engineering, Chonbuk National University, Jeonju 561-756, Korea*
[3]*Department of BIN Fusion Technology, Chonbuk National University, Jeonju 561-756, Korea*

(Received 15 May 2012; accepted 2 August 2012; published online 14 August 2012)

This paper reports on an effective chemical etching treatment to remove a boron-rich layer which has a significant negative impact on n-type silicon (Si) solar cells with boron emitter. A nitric acid-grown oxide/silicon nitride stack passivation on the boron-rich layer-etched boron emitter markedly decreases the emitter saturation current density J_{0e} from 430 to 100 fA/cm^2. This led to 1.6% increase in absolute cell efficiency including 22 mV increase in open-circuit voltage V_{oc} and 1.9 mA/cm^2 increase in short-circuit current density J_{sc}. This resulted in screen-printed large area (239 cm^2) n-type Si solar cells with efficiency of 19.0%. © *2012 American Institute of Physics*. [http://dx.doi.org/10.1063/1.4746424]

N-type silicon (Si) solar cells have become an area of active investigation because of superior electronic properties of n-type Si wafers including high bulk lifetime, high tolerance to metallic impurities, and no light-induced degradation (LID).[1–4] For these reasons, many organizations are trying to develop a cost-effective and manufacturable technology for boron-doped (p^+) emitter formation in n-type Si solar cells.[5–10] However, most of the current processes for the p^+ emitter formation result in unintentional supersaturated boron-rich layer (BRL) on top of the p^+ emitter.[11] It is conjectured that the BRL acts as high recombination site due to inactivate boron, segregated metal impurities, and structural defects which interfere with surface passivation and results in lifetime degradation.[12–15] Since both surface passivation and bulk lifetime are key to high efficiency cells, the BRL should be removed to attain high efficiency n-type Si solar cells. Oxidation of heavily boron-diffused Si, after the drive-in, is often used to remove or consume the BRL.[16] However, Macdonald and Phang reported that segregated iron (Fe) impurities in the BRL can be re-injected from the p^+ emitter into Si during the BRL oxidation.[15,17] This phenomenon can impede the development of high efficiency n-type Si solar cells because high concentration of re-injected metal impurities (e.g., Fe and Cr) can degrade bulk lifetime even in n-type Si.[18] Therefore, an alternate method for BRL removal is needed to achieve high efficiency n-type Si solar cells.

In this study, we investigated a chemical etching treatment (CET) to remove the BRL to bypass the above phenomenon. Furthermore, this paper shows a positive synergistic effect of passivating the chemically etched p^+ emitter surface with nitric acid-grown oxide (NAO) capped with plasma-enhanced chemical vapor deposition (PECVD) silicon nitride (SiN_x) to achieve high efficiency n-type Si solar cells.

In this study, an inkjet-printed paste from Honeywell Electronic Materials was used for boron diffusion and its quality was assessed in terms of emitter saturation current density (J_{0e}). For J_{0e} measurements and cell fabrication, 6 in. pseudo-square high lifetime Czochralski (Cz) n-type Si wafers with a resistivity of 5 Ω cm were used. After RCA cleaning, boron dopant source was printed on both surfaces using an inkjet printer, Fuji Dimatix DMP 2831 tool. A drive-in was performed at 950 °C for 1 h in a nitrogen (N_2) ambient followed by a 5% hydrofluoric acid (HF) dip. This resulted in a p^+ emitter sheet resistance of 45 Ω/□. Then, the wafers were divided into four groups: I, II, III, and IV, as shown in Table I. Groups I and II with the BRL were passivated by SiN_x and NAO/SiN_x stack, respectively, on both sides. Groups III and IV received CET using a mixture of nitric acid (HNO_3), glacial acetic acid (CH_3COOH), and HF for a short period to remove the BRL. After the CET, the sheet resistance of p^+ emitter increased from 45 Ω/□ to 60 Ω/□. Wafers in group III and IV were then double side passivated with SiN_x and NAO/SiN_x films. The samples for J_{0e} measurements had a symmetric structure as shown in Fig. 1(a). All the above samples, without any metallization, were subjected to a thermal cycle with a peak temperature of 750 °C in a belt furnace to simulate the firing of screen-printed contacts. The quasi-steady state photoconductivity (QSSPC) technique was used for the J_{0e} measurements.[19]

Large area (239 cm^2) n-type Si solar cells [Fig. 1(b)] were fabricated on 6 in. pseudo-square 5 Ω cm Cz n-type Si wafers. After the standard saw damage etching and chemical texturing processes, phosphorus dopants were implanted on the rear surface for making the phosphorus-doped (n^+) back surface field (BSF). A boron dopant source was deposited on the front surface using the inkjet printer. The samples were subjected to a 950 °C drive-in for 1 h in a tube furnace in a N_2 ambient. Then, the wafers were also divided into four groups for surface passivation, as shown in Table I. After the surface passivation, a conventional grid pattern on the front and a point contact pattern on the rear were screen-printed by using silver/aluminum (Ag/Al) and Ag paste, respectively. A rapid cofiring process at a peak temperature of 750 °C was used for co-firing the front and back contacts. Finally, a Ag reflector

a)Electronic mail: yok6@mail.gateh.edu.

TABLE I. J_{0e} values and cell efficiencies with different passivation scheme.

Group	Passivation scheme	J_{0e} (fA/cm^2)	V_{oc} (mV)	J_{sc} (mA/cm^2)	FF (%)	Efficiency (%)
I	SiN_x	430	622	36.7	0.76	17.4
II	NAO/SiN_x	230	626	37.3	0.77	18.0
III	CET + SiN_x	480	620	36.5	0.76	17.1
IV	CET + NAO/SiN_x	100	644	38.6	0.76	19.0

paste was screen-printed on the rear to connect the point contacts.

Microstructure and local composition of the p^+ emitter were examined using transmission electron microscopy (TEM) in conjunction with scanning transmission electron microscopy (STEM) and high resolution electron microscopy (HREM). Auger electron spectroscopy (AES) was carried out to analyze the composition of the BRL and doped regions near the surface. Chemically mirror-polished planar n-type Si wafers were used for above measurements.

Table I shows the J_{0e} values and *I-V* characteristics of the cells in groups I, II, III, and IV. A J_{0e} of 430 fA/cm^2 and efficiency of 17.4% were obtained from group I which had the BRL and only SiN_x passivation. The group II with NAO/SiN_x stack passivation on top of the BRL showed an improved J_{0e} of 230 fA/cm^2 and cell efficiency of 18.0%. To investigate the effect of BRL removal with CET on the passivation and cell performance, J_{0e} and cells in the groups III and IV were also analyzed. The group III samples with SiN_x passivation on BRL-etched p^+-Si showed a high J_{0e} of 480 fA/cm^2, which again resulted in a poor efficiency of 17.1%. This indicates that the BRL removal alone by CET is not enough to lower the J_{0e} value. The group IV samples with NAO/SiN_x passivation after the BRL removal showed a very significant improvement with a J_{0e} of 100 fA/cm^2 in conjunction with cell efficiency of 19.0%, open-circuit voltage (V_{oc}) of 644 mV, and short-circuit current (J_{sc}) of 38.6 mA/cm^2.

Internal quantum efficiency (IQE) of the finished solar cells was measured to understand the front and rear side contribution to the observed improvements in V_{oc} and J_{sc} in group IV cells. Figure 2 shows the IQE of a typical cell in each group. It shows an appreciable difference in the short wavelength range from 350 to 650 nm but almost no change in the long wavelength IQE. This suggests that the observed improvement in group IV cells is associated with the emitter and not with the bulk or BSF regions. In addition, the IQE trend in the short wavelength is consistent with measured J_{0e} values, as shown in Table I. Higher the IQE, lower the J_{0e} due to enhanced passivation. These results demonstrate that the significant improvement in group IV cell efficiency came from the increase in V_{oc} and J_{sc}, due to the improved passivation of the p^+ emitter, resulting from the combined effect of BRL removal by CET and NAO/SiN_x passivation.

To understand the reason for the significant positive impact of CET and NAO/SiN_x passivation on the cell performance, TEM measurements were employed to examine the Si surface. Figure 3 shows STEM and HREM images of the symmetric (SiN_x-NAO-p^+-n-p^+-NAO-SiN_x) samples in groups II and IV, which represent NAO/SiN_x passivated samples with and without the BRL, respectively. A very thin dark layer with periodic agglomeration, indicated by black arrow in Fig. 3(a), was observed at the Si/SiN_x interface in the case of NAO/SiN_x passivated sample with the BRL. However, NAO/SiN_x passivated p^+ emitter without BRL in Fig. 3(b) showed a very clean interface with no dark thin layer or agglomeration. These agglomerations are often associated with impurities and structural defects in the crystal lattice that can give rise to recombination centers.[20] HREM

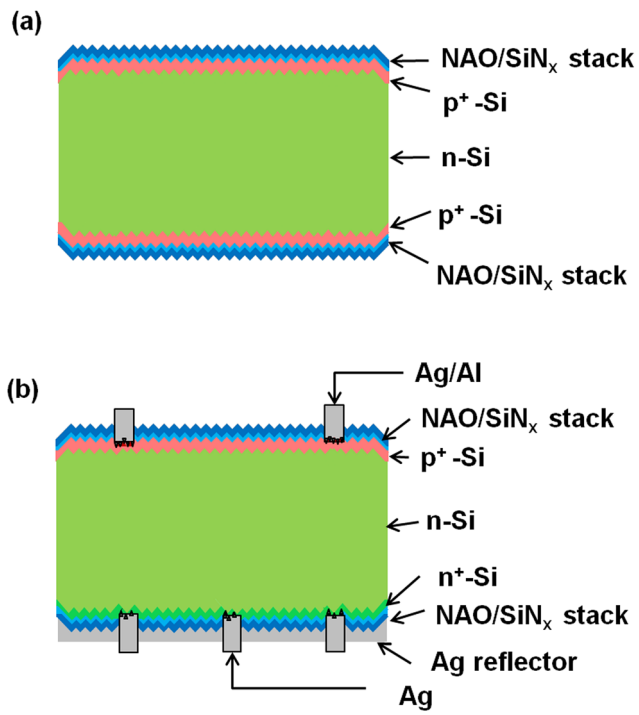

FIG. 1. Schematic layout of (a) J_{0e} sample structure and (b) n-type Si solar cell structure.

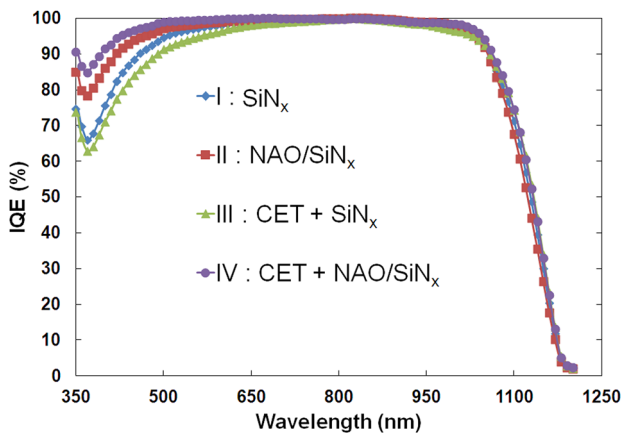

FIG. 2. IQE data of the n-type Si solar cell by using different passivation process of group I–IV.

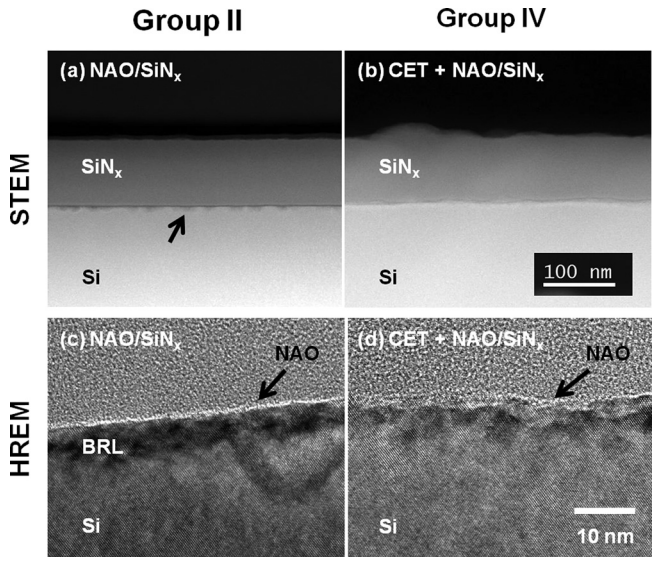

FIG. 3. STEM and HREM images obtained from the symmetric NAO/SiN_x passivated boron emitter (SiN_x-NAO-p^+-n-p^+-NAO-SiN_x) structure: (a) STEM of NAO/SIN_x passivated p^+ emitter with BRL, (b) STEM of NAO/SiN_x passivated p^+ emitter with BRL removed, (c) HREM of NAO/SiN_x passivated p^+ emitter with BRL, and (d) HREM of NAO/SiN_x passivated p^+ emitter with BRL removed.

images of the same spot are shown in Figs. 3(c) and 3(d) to magnify and quantify this observation. The sample with the BRL showed a 10 nm thick dark layer in conjunction with the agglomerated regions that were around 20–25 nm in size [Fig. 3(c)]. The sample with the BRL removed, Fig. 3(d), showed only few dark spots and hardly any agglomeration. Thus, the CET process used in this study was able to remove the thin dark layer as well as the agglomerations at the interface. Note that the NAO and SiN_x layers can be seen more clearly in the HREM images. Also, notice that a very uniform light-colored NAO layer with a thickness of 1–2 nm is observed in Fig. 3(c), whereas the BRL-etched sample in Fig. 3(d) showed a thinner oxide layer. Thus, the NAO layer morphology appears a little different on the BRL-etched p^+ emitter.

To understand the chemical composition of the interface in samples with and without the BRL, Figs. 3(c) and 3(d), AES depth profiling was performed on the above two samples. Group II sample with the BRL showed two different peaks corresponding to boron and oxygen elements at the Si interface as shown in Fig. 4(a). The boron concentration in this region was above $1 \times 10^{20}\,cm^{-3}$ because boron detection limit of the AES used in this study was about $1 \times 10^{20}\,cm^{-3}$. This was also supported by secondary ion mass spectrometry (SIMS) measurement in Ref. 9. Therefore, TEM and AES analyses combined indicate that the light thin layer and the dark thin layer with periodic agglomeration underneath [Fig. 3(c)] in group II samples correspond to Si-oxide and BRL, respectively. However, there is no notable boron peak at the interface of the group IV samples with BRL-etched emitters [Fig. 4(b)]. In addition, no oxygen peak was observed in Fig. 4(b) even though HREM was able to reveal NAO layer as shown in Fig. 3(d). It is because the NAO was too thin at this spot to be detected by AES. This demonstrates that CET was effective in removing the BRL, but it also affected the

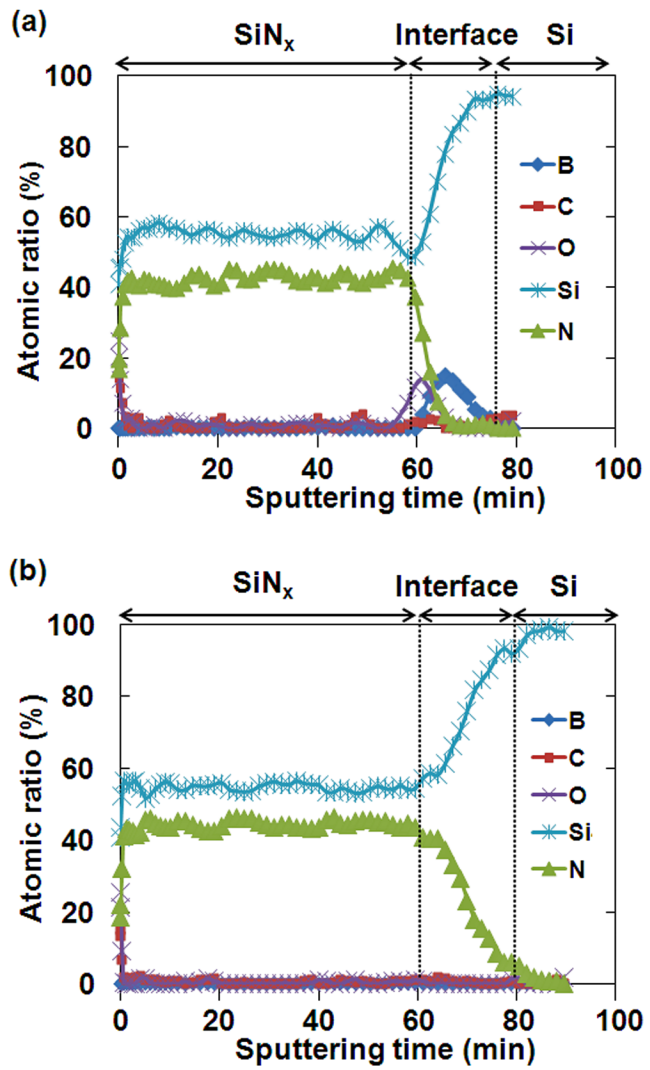

FIG. 4. AES depth profiling analysis measured from the symmetric structure sample in (a) group II and (b) group IV.

uniformity of NAO. However, the CET combined with NAO/SiN_x passivation still gave 1.6% improvement in cell efficiency.

Mihailetchi *et al.* also reported the effect of nitric acid pretreatment on the passivation of p^+ emitters formed by BBr_3 diffusion.[21] They showed that the cell efficiency increased from 15.9% to 17.9% by applying NAO/SiN_x. We saw an efficiency improvement from 17.4% to 18.0% if we apply NAO/SiN_x without removing the BRL. However, after the BRL removal and NAO/SiN_x passivation, we obtained 1.6% enhancement in an absolute efficiency even though NAO was slightly non-uniform as shown in Fig. 3(d). It is important to note that chemically etched p^+ emitter passivated with SiN_x, without NAO, gave a poor cell efficiency of 17.1% (Table I). In fact, SiN_x passivation with the BRL was slightly superior, resulting in 17.4% efficiency. Thus, PECVD SiN_x alone is not able to effectively passivate p^+ emitter, with or without the BRL. NAO/SiN_x stack on top of the BRL also failed, resulting in efficiency of 18.0%. NAO/SiN_x passivation without the BRL worked best resulting in 19.0% cell efficiency with a V_{oc} of 644 mV and a J_{sc} of 38.6 mA/cm^2. Finally, the bulk lifetime in these n-type Si solar cells was found to be 1.5 ms because the BRL was never

subjected to oxidation to avoid injection of impurities and defects in the bulk.

In summary, CET for the BRL removal and its impact on cell performance were reported in this work. It was found that SiN_x passivation, with and without the BRL, resulted in high J_{0e} values and low cell efficiency in the range of 17.1%–17.4%. However, the combination of CET and NAO/SiN_x passivation resulted in a sharp decrease in J_{0e} from 450 fA/cm^2 to 100 fA/cm^2. In addition, CET for BRL removal, instead of oxidation, preserved the high bulk lifetime. Furthermore, this process resulted in a large area (239 cm^2) Cz n-type Si solar cell with 19.0% conversion efficiency. Detailed cell analysis showed that a 1.6% increase in absolute cell efficiency, 22 mV improvement in V_{oc}, and 1.9 mA/cm^2 increase in J_{sc} resulted from a combined effect of reduced J_{0e} and increased short wavelength response.

The authors would like to thank L. Metin and H. Xu of Honeywell Electronic Materials for their cooperation. This work was supported by "Human Resource Development Program (201040100660)" of the Korea Institute of Energy Technology Evaluation and Planning (KETEP) grant and Honam Leading Industry Office through the Leading Industry Development for Economic Region (R0001244) funded by the Ministry of Knowledge Economy, Korea.

[1]J. Schmidt, A. G. Aberle, and R. Hezel, in *Proceedings of the 26th IEEE PVSC, Anaheim, CA* (IEEE, New York, 1997), p. 13.
[2]S. W. Glunz, S. Rein, J. Y. Lee, and W. Warta, J. Appl. Phys. **90**, 2397 (2001).
[3]D. Macdonald and L. J. Geerligs, Appl. Phys. Lett. **85**, 4061 (2004).
[4]J. E. Cotter, J. H. Guo, P. J. Cousins, M. D. Abbott, F. W. Chen, and K. C. Fisher, IEEE Trans. Electron Devices **53**, 1893 (2006).
[5]A. Das, K. Ryu, and A. Rohatgi, IEEE J. Photovoltaics **1**, 146 (2011).
[6]D. L. Meier, V. Chandrasekaran, H. H. Davis, A. M. Payne, W. Xiaoyan, V. Yelundur, E. O'Neill, O. Young-Woo, F. Zimbardi, and A. Rohatgi, IEEE J. Photovoltaics **1**, 123 (2011).
[7]B. J. Pawlak, T. Janssens, S. Singh, I. Kuzma-Filipek, J. Robbelein, N. E. Posthuma, J. Poortmans, F. Cristiano, and E. M. Bazizi, Prog. Photovoltaics **20**, 106 (2012).
[8]A. Rohatgi, D. L. Meier, B. McPherson, Y.-W. Ok, A. D. Upadhyaya, J.-H. Lai, and F. Zimbardi, Energy Procedia **15**, 10 (2012).
[9]K. Ryu, A. Upadhyaya, Y.-W. Ok, M. H. Kang, V. Upadhyaya, L. Metin, H. Xu, A. Bhanap, and A. Rohatgi, IEEE Electron Device Lett. **33**, 854 (2012).
[10]K. Ryu, A. Upadhyaya, Y.-W. Ok, V. Upadhyaya, L. Metin, H. Xu, A. Bhanap, and A. Rohatgi, "High efficiency n-type solar cells with screen-printed boron emitters and ion-implanted back surface field," in *Proceedings of the 38th IEEE PVSC, Austin, TX, 2012* (IEEE, to be published).
[11]S. M. Myers, M. Seibt, and W. Schroter, J. Appl. Phys. **88**, 3795 (2000).
[12]X. J. Ning, J. Electrochem. Soc. **143**, 3389 (1996).
[13]P. J. Cousins and J. E. Cotter, IEEE Trans. Electron Devices **53**, 457 (2006).
[14]M. A. Kessler, T. Ohrdes, B. Wolpensinger, and N. P. Harder, Semicond. Sci. Technol. **25**, 055001 (2010).
[15]D. Macdonald, H. Mackel, and A. Cuevas, in *Proceedings of the IEEE 4th World Conference on Photovoltaic Energy Conversion, Waikoloa, HI* (IEEE, New York, 2006), p. 952.
[16]J. Libal, R. Petres, T. Buck, R. Kopecek, G. Hahn, R. Ferre, M. Vetter, I. Martin, K. Wambach, I. Roever, and P. Fath, in *Proceedings of 20th European Photovoltaic Solar Energy Conference, Barcelona* (WIP, Munich, 2005), p. 793.
[17]S. P. Phang and D. Macdonald, J. Appl. Phys. **109**, 073521 (2011).
[18]J. Schmidt, K. Bothe, R. Bock, C. Schmiga, R. Krain, and R. Brendel, in *Proceedings of 22nd European Photovoltaic Solar Energy Conference, Milan* (WIP, Munich, 2007), p. 998.
[19]R. R. King and R. M. Swanson, IEEE Trans. Electron Devices **38**, 1399 (1991).
[20]A. A. Istratov, T. Buonassisi, R. McDonald, A. Smith, R. Schindler, J. Rand, J. P. Kalejs, and E. R. Weber, J. Appl. Phys. **94**, 6552 (2003).
[21]V. D. Mihailetchi, Y. Komatsu, and L. Geerligs, Appl. Phys. Lett. **92**, 063510 (2008).